JOURNAL OF VIROLOGY, Nov. 1995, p. 7138–7146 Vol. 69, No. 11
0022-538X/95/$04.00+0

Frequent Disruption of the *Nf1* Gene by a Novel Murine AIDS Virus-Related Provirus in BXH-2 Murine Myeloid Lymphomas

BRIAN C. CHO,[1]† JOHN D. SHAUGHNESSY, JR.,[1] DAVID A. LARGAESPADA,[1]
HENDRICK G. BEDIGIAN,[2] ARTHUR M. BUCHBERG,[3]
NANCY A. JENKINS,[1] AND NEAL G. COPELAND[1]*

Mammalian Genetics Laboratory, ABL-Basic Research Program, NCI-Frederick Cancer Research and Development Center, Frederick, Maryland 21702[1]; The Jackson Laboratory, Bar Harbor, Maine 04609[2]; and Department of Microbiology and Immunology, Jefferson Medical College, Philadelphia, Pennsylvania 19107[3]

Received 26 May 1995/Accepted 15 August 1995

***Evi-2*, a common site of viral integration in BXH-2 myeloid lymphomas, is located within a large intron of the *Nf1* tumor suppressor gene. Viral integration at *Evi-2* appears to induce disease by disrupting normal *Nf1* expression. During our attempts to characterize the nature of the proviruses located at *Evi-2*, we found that approximately half of the proviruses were defective nonecotropic proviruses (A. M. Buchberg, H. G. Bedigian, N. A. Jenkins, and N. G. Copeland, Mol. Cell. Biol. 10:4658–4666, 1990). This was surprising, since most proviruses characterized at other BXH-2 common integration sites are full-length ecotropic viruses. In the studies described here, we found that this defective provirus carries two large deletions, one in *pol* and one in *env*, and is structurally related to another murine retrovirus, the murine AIDS retrovirus. By using oligonucleotide probes specific for this defective provirus, designated MRV, we showed that MRV-related proviruses are carried as endogenous germ line proviruses in most inbred strains. In addition, we identified the endogenous MRV provirus that gives rise to the defective proviruses identified at *Evi-2*. We present a model that accounts for the positive selection of MRV proviruses at *Evi-2*, which may allow selective identification of common viral integration sites harboring tumor suppressor genes.**

BXH-2 mice have the highest incidence of spontaneous retrovirally induced myeloid leukemia of any known inbred strain and, as such, represent a valuable model system for identifying novel myeloid disease genes (3). BXH-2 is a recombinant inbred strain derived from a cross between C57BL/6J and C3H/HeJ mice (5). Although the leukemia incidence in the two parental strains is low, greater than 95% of BXH-2 mice die of myelomonocytic leukemia by 1 year of age (3, 22). The high incidence of myeloid leukemia in BXH-2 mice is causally associated with the expression of a B-ecotropic murine leukemia virus (MuLV) that is horizontally transmitted in this strain (4, 26).

Chronic MuLVs, such as ecotropic viruses, induce disease by insertional activation or alteration of cellular proto-oncogenes or by insertional inactivation of tumor suppressor genes (reviewed in references 6, 25, 32, 37, and 52). The disease genes that are affected by viral integration are initially identified as common viral integration sites in tumor DNAs. One common viral integration site that has been identified in BXH-2 myeloid tumors is *Evi-2* (ecotropic viral integration site 2) (7). The *Evi-2* locus is located within a large intron of the neurofibromatosis type 1 (*Nf1*) gene (35, 53). *Nf1* is a tumor suppressor gene that has been shown to function as a mammalian GTPase-activating protein (reviewed in reference 19). Proteins with GTPase-activating activity catalyze the exchange of GDP for GTP on Ras. Since Ras is active only in the GTP-bound state, one normal function of the Nf1 protein appears to be as a negative regulator of Ras.

Mutations in the human *Nf1* gene produce a variety of clinical features, the most notable of which are hyperpigmented patches on the skin (cafe-au-lait spots) and neurofibromas (19). Neurofibromas are benign polyclonal tumors which are composed of a variety of cell types, including Schwann cells and fibroblasts. Patients with neurofibromatosis type 1 are also at increased risk for developing a variety of frank malignancies. In addition, juvenile patients with neurofibromatosis type 1 have a greatly increased incidence of myeloid leukemia, including juvenile chronic myelogenous leukemia and monosomy 7 syndrome (46). Bone marrow samples from children with neurofibromatosis type 1 who develop malignant myeloid disorders show loss of heterozygosity at the *Nf1* locus, and the *Nf1* allele that is retained in the tumor is the one inherited from the parent with neurofibromatosis type 1. The normal *Nf1* allele is deleted (45). These results strongly suggest that mutations in the human *Nf1* gene predispose to the development of myeloid disease.

On the basis of results obtained with human juvenile patients with neurofibromatosis type 1 it has been speculated that viral integration at *Evi-2* induces myeloid disease by preventing the production of a functional Nf1 protein. Consistent with this prediction, about 30% of BXH-2 tumors with viral integrations at *Evi-2* have viral integrations in both *Nf1* alleles (7, 32). This pattern of biallelic integration would be expected for a tumor suppressor gene in which both alleles must be mutated for tumor formation to occur. For tumor suppressor genes with only one viral integration, it is possible that the second allele is mutated by a spontaneous nonviral event such as a small deletion or point mutation.

Characterization of a large number of proviruses located at *Evi-2* produced an unexpected result (7). Approximately half of the proviruses (6 of 14) appeared to represent a deleted provirus that is about 5.3 kb long. The deletion included at least part of the *env* gene in addition to other, undetermined viral sequences. This result was surprising since proviruses located at other common viral integration sites in BXH-2 my-

* Corresponding author. Phone: (301) 846-1260. Fax: (301) 846-6666. Electronic mail address: copeland@ncifcrf.gov.
† Present address: Department of Microbiology and Immunology, Jefferson Medical College, Philadelphia, PA 19107.

eloid tumors are primarily full-length ecotropic proviruses, which is consistent with the postulated causative role of ecotropic viruses in BXH-2 disease. It appears, therefore, that there is something special about the *Evi-2* common integration site that selects for the presence of this defective provirus. In the studies described here, we cloned and characterized one of these defective proviruses. We also generated oligonucleotide probes specific for this defective provirus and used them to examine the origin of this defective provirus. The results of these studies indicate that this defective provirus is carried in the BXH-2 germ line as a single-copy endogenous provirus and is presumably transmitted to tumor cells following rescue by an ecotropic virus helper. Interestingly, sequence analysis has indicated that this defective provirus is closely related to the murine AIDS (MAIDS) virus (2, 11). Inoculation of mice with the MAIDS virus induces an immunodeficiency disease with striking similarities to human AIDS.

MATERIALS AND METHODS

Preparation and analysis of genomic DNA. High-molecular-weight genomic DNA was prepared and analyzed by Southern blotting. *Evi-2*-specific probe D (7) and an MuLV U3 long terminal repeat (LTR)-specific probe (40) were labeled by random priming with the Prime It kit (Stratagene). For "unblot analysis" (hybridization to dried gels), the procedure of Tsao et al. (50) was followed with minor modifications. Briefly, 10 μg of restriction endonuclease-digested DNA was separated on a 0.8% agarose gel, dried under vacuum for 1.5 h at 50°C, and hybridized for 6 h at 65°C (Δpol) or 55°C (Δenv) in 6× SSCP (1× SSCP is 87.7 g of NaCl, 44.1 g of sodium citrate, and 0.0375 g of citric acid in 500 ml)–5× Denhardt's solution–1% bovine serum albumin–0.5% sodium dodecyl sulfate (SDS)–0.05% sodium phosphate–10 mg of denatured salmon sperm DNA per ml. Oligonucleotide probes (Δenv and Δpol) were labeled with [γ-^{32}P]ATP by using polynucleotide kinase (New England Biolabs). Washes were done at high stringency (1× SSCP) for 15 min or at lower stringency (5×, 3×, or 2× SSCP). Probes were stripped from the dried gels by alkali denaturation for reuse (41). Southern blots (or dried gels) were subjected to autoradiography with Kodak XAR-5 film and two intensifying screens (Dupont). Autoradiography was done at −70°C for 1 to 10 days.

Construction and screening of subgenomic, size-selected λ libraries. BXH-2 spleen DNA from animal 82-60 was digested with *Eco*RI and electrophoresed through a 0.8% agarose gel. Fractions of DNA in the 14-kb size range were purified as follows. Agarose slices were homogenized and incubated with 200 μl of phenol and subsequently incubated in a dry-ice–ethanol bath for 12 min. The tubes were spun at 4°C in an Eppendorf microcentrifuge for 15 min, and the aqueous phase was removed. A 200-μl volume of TE (10 mM Tris-Cl [pH 8.0], 1 mM EDTA [pH 8.0]) was added to each phenol-agarose mixture and vortexed prior to another 15 min of spinning at 4°C. The two aqueous phases from each gel slice were pooled and subjected to phenol extraction and two chloroform extractions. Sodium acetate was then added to a final concentration of 300 mM before ethanol precipitation. The pellets were dried in a vacuum centrifuge and resuspended in TE. The fractions were subjected to Southern blot analysis with *Evi-2*-specific probe D (7) and the U3 LTR probe. The fraction most enriched for the defective *Evi-2* provirus was ligated to λ DASH *Eco*RI arms and packaged with Gigapack Gold Plus as recommended by the manufacturer (Stratagene). Approximately 8.4×10^5 recombinant phage were screened (41) with probe D, the U3 LTR probe, and an ecotropic virus-specific *env* probe (9). Of 49 clones, 1 that hybridized to probe D and the U3 LTR probe but not to the envelope probe was selected and purified for further analysis.

Germ line *Mrv1* was cloned from BXH-2 cell line B114 (32). High-molecular-weight DNA from B114 was digested with *Eco*RI and electrophoresed through a 0.8% low-melting-point agarose gel. Fractions of DNA in the 10-kb size range were purified as previously described (47). The fraction containing the *Mrv1* provirus was ligated to λ DASH *Eco*RI arms and packaged with Gigapack Gold Plus as recommended by the manufacturer (Stratagene). Approximately 8.4×10^5 recombinant phage were screened with a 42-bp PCR-generated probe specific for the *Mrv1* envelope deletion. Briefly, the 42-bp probe, which contains exactly 21 bp from the 5′ and 3′ sides of the *Mrv1* envelope deletion, was generated from pΔMLV, a plasmid subclone containing the defective *Evi-2* provirus (see Results). This fragment was gel purified and used as a template for the production of a discrete high-specific-activity DNA probe by PCR by a modification of the method of Schowalter and Summer (43). Of 10 positive clones, 1 was plaque purified and subcloned into plasmid KS(+) (Stratagene). This clone was designated p*Mrv1*.

DNA sequencing. The pΔMLV plasmid subclones were sequenced in accordance with the double-stranded dideoxy-chain termination method (42) by using the Sequenase version 2.0 and Taquence kits (United States Biochemical Corporation). The complete nucleotide sequence of both DNA strands was determined. The p*Mrv1* plasmid subclone was sequenced with the PRISM ready-reaction dyedeoxy terminator cycle sequencing kit (Perkin Elmer). The sequencing reactions were run on a 373A automated sequencing apparatus in accordance with the manufacturer's (Applied Biosystems) protocol. The complete nucleotide sequence of both DNA strands from both pΔMLV and germ line p*Mrv1* was determined.

Oligonucleotide synthesis. All sequencing primers and oligonucleotide probes were synthesized on an Applied Biosystems 380B DNA synthesizer. The Δpol probe is a 39-mer (GGGAGGTCAGGGTCAGAAGTCCTCCATGATTGCC TCGAG), the Δenv probe is a 26-mer (GTCTTCAATGTTACAAGGGTGG TTTG), and the U3 LTR probe is a 22mer (ATTAACAGTTACAAATCA AGGC). The primers used to generate the 42-bp *Mrv1* envelope deletion-specific PCR probe were CCTCACCAGGTCTT and ACAGTCTCTCAAACC. Sequences are shown in the 5′-to-3′ orientation.

Computer-assisted sequence analysis. Nucleotide and protein sequence analysis was performed on a VAX 8600 with the Genetics Computer Group software package (14). All available databases were searched for related sequences. Sequence comparisons and alignments were done with the programs GAP, Pileup, and Prettyplot.

RESULTS

Cloning and sequence analysis of a defective provirus from the *Evi-2* locus. As a first step in characterizing the defective provirus identified at *Evi-2*, we cloned one of these proviruses from BXH-2 tumor 82-60 (7). Briefly, tumor DNA was digested with *Eco*RI, an enzyme that does not cleave the defective provirus, and a 13.7-kb fragment containing the provirus and 5′ and 3′ *Evi-2*-flanking DNA was cloned in λ DASH. Positive λ clones were recognized by virtue of their hybridization to a genomic *Evi-2* probe and to an ecotropic MuLV LTR probe and by their failure to hybridize with an ecotropic MuLV *env* probe (data not shown). The 13.7-kb fragment was then subcloned into the *Eco*RI site of pBluescript II KS+. This subclone was designated pΔMLV. Finally, the pΔMLV subclone was cleaved with *Pst*I, an enzyme that cleaves the defective provirus once in each proviral LTR, and a 5.2-kb virus-containing fragment was cloned into the *Pst*I site of pBluescript II KS+. This subclone was designated pΔSC. Subclones pΔMLV and pΔSC were then sequenced by the double-stranded dideoxy-chain termination method (42). The complete nucleotide sequence of both strands of the provirus was determined (Fig. 1).

Nucleotide sequence comparisons indicate that the defective virus is 4,765 bp long and has suffered two large deletions relative to wild-type MuLV (20). One of the deletions is in *pol*, and the other is in *env* (Fig. 2). The *pol* deletion is 1,812 bp long and includes the 5′ half of *pol*. The *env* deletion is 1,567 bp long and includes the 3′ end of gp70 and the 5′ end of p15E. Both deleted regions are flanked by direct repeats in the wild-type virus and are present only once at the site of the deletion in the defective viral genome (Fig. 1). Similar deletions are carried by another defective virus, the MAIDS virus (2, 11). The MAIDS virus also demonstrates high sequence homology throughout the *gag*, *pol*, and *env* genes with the defective *Evi-2* provirus (data not shown), and both viruses encode a complete *gag* open reading frame (Fig. 3). Because of the relatedness of these two viruses, we designated the defective *Evi-2* virus the MAIDS virus-related virus (MRV).

Many features of MRV, however, distinguish it from the MAIDS virus. The MAIDS virus has suffered a number of small deletions in *pol* and *env* that are not present in MRV (Fig. 2). The restriction maps of MRV and the MAIDS virus are also relatively divergent (Fig. 2), as are the C-terminal p15^{gag} and p12^{gag} coding regions (Fig. 3). Finally, nucleotide sequence comparisons show that the MRV LTR is xenotropic virus related (36) while the MAIDS virus LTR is ecotropic virus related (data not shown).

Inbred mouse strains carry endogenous MRV-related loci. To determine if inbred mouse strains carry endogenous MRV-

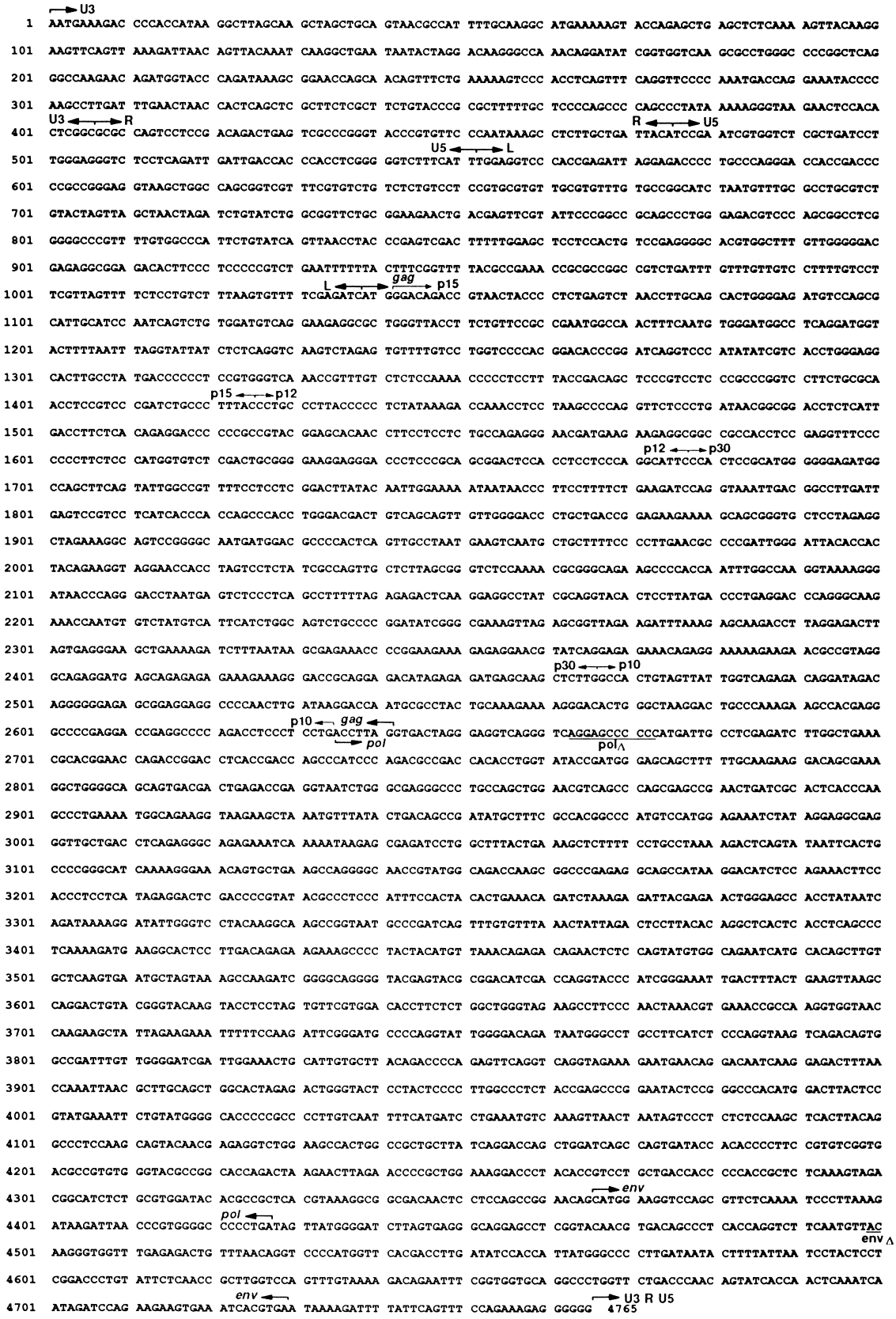

FIG. 1. Nucleotide sequence of the cloned defective *Evi-2* provirus. The LTR (U3, R, and U5), leader, and structural gene boundaries are indicated by arrows. Potential *gag* products are also delineated with arrows. Underlined sequences indicate the regions where the two large deletions occurred. Underlined sequences are present in wild-type virus as direct repeats and flank the deleted region. Numbers to the left and right indicate the positions of the adjacent nucleotides.

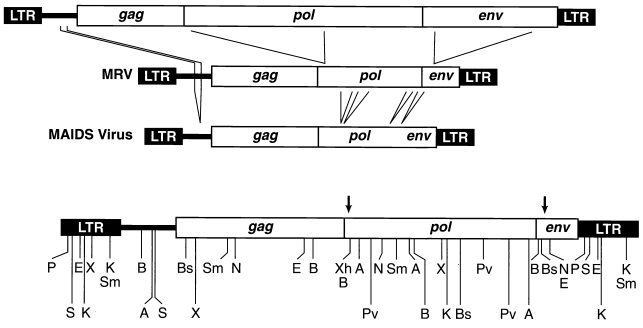

FIG. 2. MRV and the MAIDS virus encode large deletions in *pol* and *env*. A comparison of the proviral structures of the MAIDS B-ecotropic helper virus (BM5; 11), MRV, and the MAIDS virus (BM5d; 11) is shown at the top. The lines between the viruses represent the approximate regions deleted. Only relatively large deletions are shown; very small deletions have not been included. An MRV restriction map for enzymes that have been used to characterize the MAIDS virus is shown at the bottom. Restriction enzyme abbreviations: A, *Acc*I; B, *Bgl*II; Bs, *Bst*EII; E, *Eco*RV; K, *Kpn*I; N, *Nco*I; P, *Pst*I; Pv, *Pvu*II; S, *Sac*I; Sm, *Sma*I; X, *Xba*I; and Xh, *Xho*I. Restriction sites located on the bottom line are not present in the MAIDS virus. The two arrows above the virus represent the deletion breakpoints.

related proviruses that may be the source of the defective provirus identified at *Evi-2*, we created synthetic oligonucleotide probes that symmetrically spanned the two MRV deletion breakpoints and specifically recognized the defective provirus at *Evi-2*. The *pol* probe (Δpol) was 39 bp long and contained three nucleotide mismatches that were introduced into the probe to prevent nonspecific hybridization caused by the high G · C content of the *pol* direct repeat. The *env* probe (Δenv) was 26 bp long and contained no nucleotide mismatches. Each

FIG. 3. Amino acid sequence comparisons of the *gag* genes of the B-ecotropic MAIDS helper virus (Eco), the MAIDS virus (Maids), and MRV (Mrv). The Genetics Computer Group programs Pileup and Prettyplot were used for alignment and identity, respectively. Boxed amino acids indicate regions of identity or conservation between MRV and either the MAIDS virus or the MAIDS B-ecotropic helper virus, while dashes are used for optimal alignment. The proteolytic products of *gag*, including p15, p12, p30, and p10, are delineated with arrows. Numbers to the right indicate the positions of the adjacent amino acids.

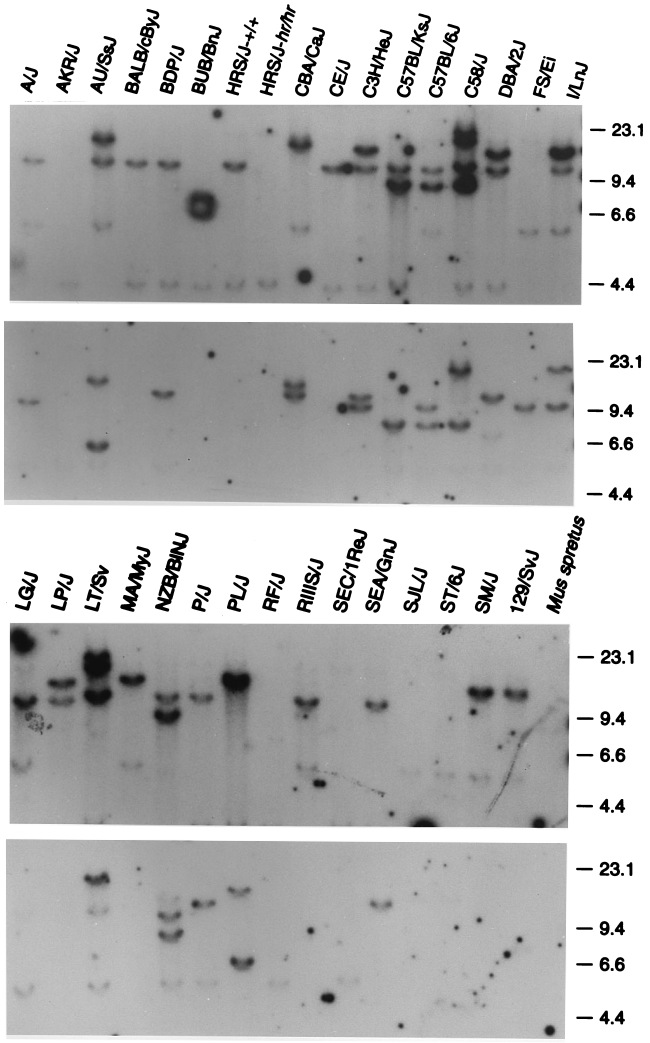

FIG. 4. Inbred mouse strains carry endogenous MRV-related loci. Inbred strain DNAs were digested with *Eco*RI and electrophoresed through 0.8% agarose gels. The gels were dried and hybridized with the Δenv probe (top) and then stripped and rehybridized with the Δpol probe (bottom). Numbers to the right are molecular size markers expressed in kilobases. Note that the weaker hybridizing *env* mutant fragments were not detected under more stringent hybridization and wash conditions (data not shown) and therefore appear to represent cross-hybridization to a more divergent set of proviruses.

probe was then hybridized to unblots (see Materials and Methods) containing *Eco*RI-digested DNAs from 33 inbred mouse strains and substrains (Fig. 4). If both probes recognized the same-size restriction fragment, this was taken as preliminary evidence that a single provirus carries both deletions (*env* and *pol*).

Strains AKR/J, BUB/BnJ, HRS/J-*hr*/*hr*, RF/J, SEC/1ReJ, SJL/J, and ST/bJ and *Mus spretus* did not carry endogenous viral loci that hybridized with either the Δpol or Δenv probe, whereas 25 strains carried at least one endogenous viral locus that hybridized with one of the two probes (Fig. 4). HRS/J-+/+ mice carry an endogenous MRV-related provirus that is not carried by HRS/J-*hr*/*hr* mice (Fig. 4). This provirus appears to represent a Y-linked provirus that is carried on many inbred strain Y chromosomes (see below). Only 8 of the 25 strains, AU/SsJ, CBA/CaJ, C57BL/KsJ, C57BL/6J, C58/J, I/LnJ, LT/Sv, and NZB/B1NJ, appeared to carry a provirus with deletions

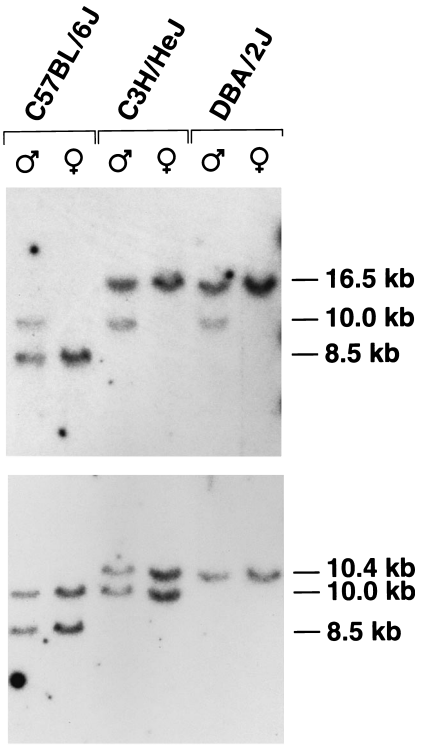

FIG. 5. Unblot analysis of MRV-related proviruses carried by male and female C57BL/6J, C3H/HeJ, and DBA/2J mice. DNAs were digested with *Eco*RI and hybridized with the Δenv probe (top). A similar blot was also hybridized with the Δpol probe (bottom).

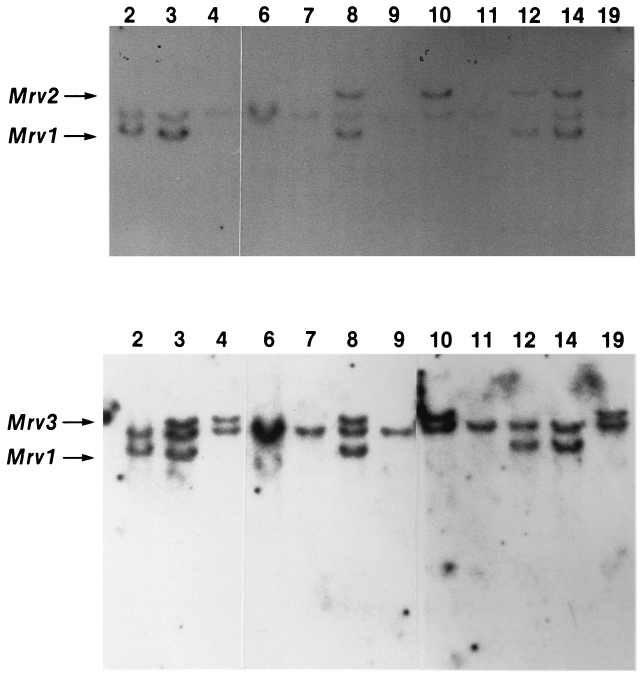

FIG. 6. Segregation of *Mrv* loci in BXH RI strains. Genomic DNAs from 12 BXH RI strains were digested with *Eco*RI and subjected to unblot analysis with the Δenv (top) and Δpol (bottom) probes. Lane numbers correspond to BXH RI strain numbers.

in both *pol* and *env* (Fig. 4). Finally, the proviruses seem to be located at many different sites within inbred-strain DNAs (as judged by the sizes of hybridizing MRV-related *Eco*RI restriction fragments) and their copy number is low. These results suggest that these endogenous loci were recently acquired in the mouse germ line and are relatively mobile in mouse chromosomes. This finding was surprising since these proviruses are replication defective because of the deletions in *pol* and *env* (18).

We were particularly interested in characterizing the *Mrv*-related loci carried by C57BL/6J and C3H/HeJ mice since these are the two progenitors of the BXH RI strains. Hybridization of *Eco*RI-digested male and female C57BL/6J and C3H/HeJ DNAs with the Δenv and Δpol probes identified five MAIDS-related proviruses (Fig. 5). One provirus, identified as a 10.0-kb *env* mutant fragment, was identified only in male DNA (Fig. 5). This provirus therefore appears to be located on the Y chromosome. A 10.0-kb *pol* mutant fragment was also identified when a similar blot was hybridized with the Δpol probe; however, the 10.0-kb *pol* mutant fragment was present in both male and female DNAs (Fig. 5). The hybridization intensities of the male and female 10.0-kb *pol* mutant fragments appeared to be equal when corrected for DNA loading (data not shown). These results suggest that there are actually two 10.0-kb proviruses; one provirus is an *env* mutant and is carried on the Y chromosome, while the other provirus is a *pol* mutant and is presumably carried on an autosome. Finally, C57BL/6J mice carry an 8.5-kb *env pol* mutant provirus that is not carried by C3H/HeJ mice, while C3H/HeJ mice carry a 16.5-kb *env* mutant provirus and a 10.4-kb *pol* mutant provirus not carried by C57BL/6J mice.

Chromosomal mapping of C57BL/6J and C3H/HeJ MRV-related loci. The C57BL/6J and C3H/HeJ MRV-related loci were initially mapped by recombinant inbred (RI) analysis with the BXH RI strains. The 8.5-kb C57BL/6J-specific *env pol* mutant provirus was mapped to chromosome 4 with both the Δenv and Δpol probes (Fig. 6 to 8 and Table 1) and was designated *Mrv1* (MAIDS-related viral locus 1). Likewise, the 16.5-kb C3H/HeJ *env* mutant provirus was mapped to chromosome 2 (*Mrv2*) and the 10.4-kb C3H/HeJ *pol* mutant provirus was mapped to chromosome 18 (*Mrv3*). The 10.0-kb *pol* mutant provirus could not be mapped in the BXH RI strains since it is carried by both C3H/HeJ and C57BL/6J mice.

The 10.0-kb *pol* mutant provirus was mapped by using the BXD (C57BL/6J × DBA/2J) RI strains (Fig. 7 and 8 and Table 2). DBA/2J mice carry a single 10.4-kb *pol* mutant provirus (*Mrv3*; Fig. 5), which is separable from the 10.0 kb *pol* mutant provirus (designated *Mrv4*) and 8.5-kb *env pol* mutant (*Mrv1*) proviruses carried by C57BL/6J mice (Fig. 8). The 10.0-kb *pol* mutant provirus mapped to chromosome 5 (Table 2 and Fig. 7). In addition, the map locations of *Mrv1* and *Mrv3*, determined in the BXD RI strains, were consistent with their map locations determined in the BXH RI strains (Table 2 and Fig. 7).

Three of the four *Mrv* loci cosegregated with already mapped endogenous proviruses (Fig. 7), raising the possibility that they represent previously identified viral loci. The xenotropic MuLV (*Xmv*) and modified polytropic MuLV (*Mpmv*) proviruses were mapped with probes from the *env* region (16, 17). *Mrv3* and *Mrv4* do not react with the Δenv probe and may contain an intact *env* gene. *Mrv3* and *Mrv4* are also carried by the same inbred mouse strains as *Xmv29* and *Xmv17*, respectively (16). It is possible, therefore, that *Mrv3* and *Mrv4* represent already mapped proviruses. The probe used to map *Xmmv23* shows 91.4% identity to MRV over a 200-bp overlapping region (data not shown). However, *Mrv1* is unlikely to represent *Xmmv23*, as C57BL6/J mice carry *Mrv1* but lack *Xmmv23* (13).

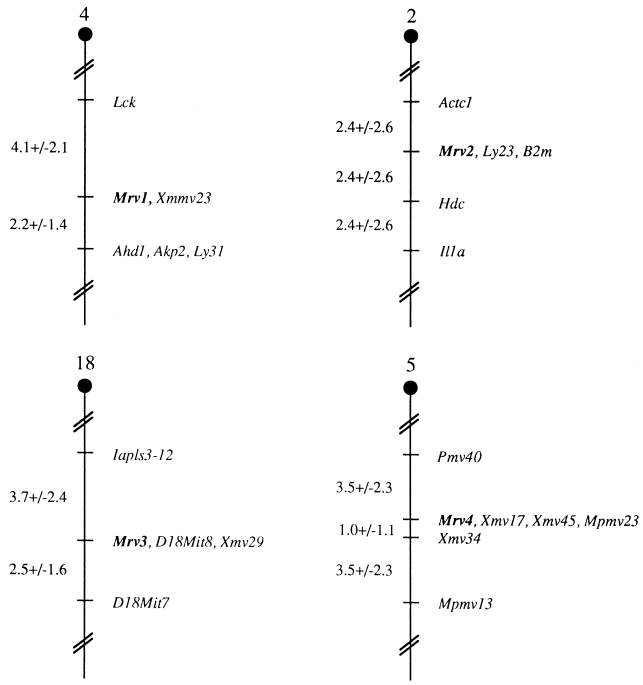

FIG. 7. Chromosomal locations of *Mrv* loci. Partial chromosome linkage maps showing the approximate map locations of *Mrv1* to *Mrv4*. Map locations were determined with RI Manager v2.5.2 (34), from the data reported in Tables 1 and 2, by using the linkage statistics developed by Silver (48). Mean interlocus distances in centrimorgans (± the standard errors) are shown to the left of each chromosome map.

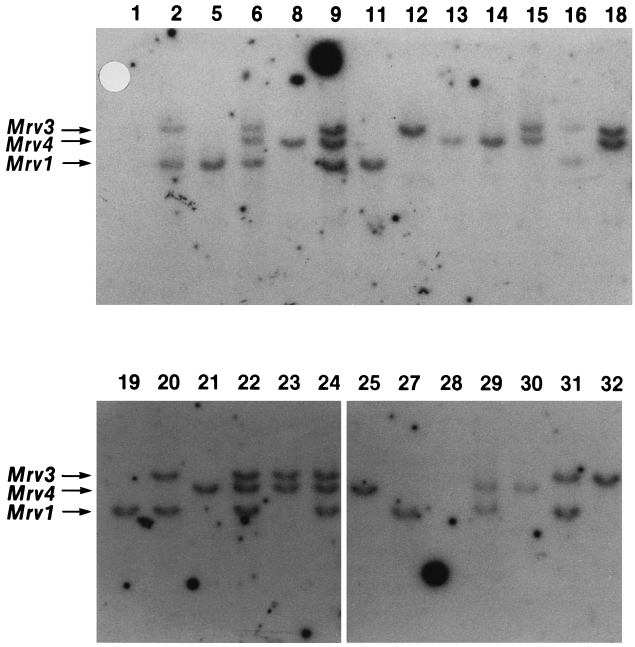

FIG. 8. Segregation of *Mrv* loci in BXD RI strains. Genomic DNAs from 26 BXD RI strains were digested with *Eco*RI and subjected to unblot analysis with the Δpol probe. Lane numbers correspond to BXD RI strain numbers.

Origin of the Y chromosome-linked *Mrv*-related provirus. The Y chromosome-linked *Mrv*-related provirus, designated *Mrv5* (Fig. 5), appears to be widely distributed among inbred-strain Y chromosomes. Analysis of male and female DNAs from 29 inbred mouse strains identified only 5 strains that did not carry *Mrv5* (Table 3). Inbred mouse strains are derived from a minimum of six male mice belonging to two distinct subspecies, *M. musculus* and *M. domesticus* (51). Interestingly, all strains carrying *Mrv5* have previously been shown to transmit an *M. musculus* Y chromosome while four of the five strains that lack *Mrv5* transmit an *M. domesticus* Y chromosome (51). These results suggest that *Mrv5* was introduced into inbred strains by one or more *M. musculus* male mice. The single exceptional strain is C57BL/10J (Table 3). These mice carry an *M. musculus* Y chromosome, yet they do not transmit *Mrv5*. This was surprising since all C57BL substrains, as well as C57L and C57BR, were derived from the mating of female 57 with male 52 from Miss Abbie Lathrop's stock and C57BL/6J, C57L/J, and C57BR/cdJ mice transmit *Mrv5* (Table 3). It is therefore likely that C57BL/10J mice originally carried *Mrv5* but it was lost during subsequent substrain propagation, possibly by homologous recombination across the LTRs.

Cloning and sequence analysis of *Mrv1*. All of the defective proviruses characterized at *Evi-2* have been found to hybridize with both the Δpol and Δenv probes, indicating that they are all derived from a common *env pol* mutant progenitor (12b). Since *Mrv1* is the only BXH-2 endogenous *Mrv* locus that carries both *env* and *pol* deletions, this result suggests that the defective proviruses characterized at *Evi-2* are, at least in part, derived from *Mrv1*. To determine if this is the case, we cloned and sequenced *Mrv1* (see Materials and Methods). As predicted, the defective *Evi-2* proviruses are derived from *Mrv1* as the sequences of *Mrv1* and the defective *Evi-2* provirus are identical except for a C-to-T change at position 559 in the *Mrv1* sequence (Fig. 1).

Retroviral replication is error prone (15). The sequence identity between *Mrv1* and the defective *Evi-2* provirus, shown here, suggests that few replication cycles separate the two proviruses. This sequence similarity also suggests that the *Mrv1* virus is not vertically transmitted in the BXH-2 strain, in contrast to the B-ecotropic virus, since this should rapidly lead to sequence divergence between the two proviruses.

Transmission of the *Mrv1*-encoded virus to myeloid tumor cells likely involves rescue of *Mrv1* by a B-ecotropic virus,

TABLE 1. Strain distribution pattern of C57BL/6J and C3H/HeJ MRV-related loci[a]

Locus	Chromosome	Strain of origin	Provirus mutation(s)	Origin of locus in BXH RI strain:												
				2	3	4	5	6	7	8	9	10	11	12	14	19
Mrv1	4	B	*env pol*	B	B	H	B	H	H	B	H	H	H	B	B	H
Mrv2	2	H	*env*	B	B	B	H	B	B	H	B	H	B	H	H	B
Mrv3	18	H	*pol*	B	H	H	H	B	B	H	B	H	B	B	B	H

[a] B, C57BL/6J; H, C3H/HeJ.

TABLE 2. Strain distribution pattern of C57BL/6J and DBA/25J MRV-related loci[a]

Locus	Chromosome	Strain of origin	Provirus mutation(s)	Origin of locus in BXD RI strain:																								
				1	2	5	6	8	9	11	12	13	14	15	16	18	19	20	21	22	23	24	25	27	28	29	30	31	32
Mrv1	4	B	*env pol*	D	B	B	B	D	B	B	D	D	D	D	B	D	B	B	D	B	D	B	D	B	D	B	D	B	D
Mrv3	18	D	*pol*	B	D	B	D	B	D	B	D	B	B	D	D	D	B	D	B	D	D	D	B	B	B	B	B	D	D
Mrv4	5	B	*pol*	D	D	D	B	B	B	D	D	B	B	B	D	B	D	D	B	B	B	B	B	D	D	B	B	D	D

[a] B, C57BL/6J; D, DBA/2J.

which is predicted to occur only rarely. Since the *Mrv1*-encoded virus does not appear to be vertically transmitted in the BXH-2 strain, *Mrv1* rescue likely occurs de novo in each animal harboring somatic *Mrv1*s. This may explain why only 12% of BXH-2 tumors harbor somatic *Mrv1*s (12a). It may also explain why the few BXH-2 tumors that carry somatic *Mrv1* proviruses often harbor multiple somatic *Mrv1* proviruses, since virus rescue, and not virus replication, may be the rate-limiting step in the formation of tumors with somatic *Mrv1*s (12a). If this hypothesis is correct, why have no other *Mrv*-related proviruses or proviruses derived from other defective endogenous proviral families (1, 19, 38) been identified at *Evi-2*? While a number of explanations are possible, one likely explanation is that *Mrv1* is expressed in a cell type that is susceptible to infection by the B-ecotropic virus helper.

DISCUSSION

Approximately half of the proviruses characterized at *Evi-2* represent defective nonecotropic proviruses (7). This was surprising since most proviruses located at other BXH-2 common viral integration sites represent full-length ecotropic MuLVs. To more fully characterize this defective provirus, we cloned and sequenced one of the defective proviruses from BXH-2 tumor DNA. Sequence analysis indicated that the defective provirus carries two large deletions, a 1.8-kb deletion in *pol* and a 1.6-kb deletion in *env*. Similar deletions have been identified in another murine retrovirus, the MAIDS virus (2, 11). Because of the structural similarity between these two viruses, we designated the defective *Evi-2* virus MRV.

Unblot analysis with oligonucleotide probes that span the MRV *env* and *pol* deletions showed that most (25 of 33) inbred mouse strains carry endogenous MRV-related proviruses. However, most of these MRV-related proviruses have a deletion in only *env* or *pol*; only 8 of 33 strains tested carried proviruses with both deletions.

Unblot analysis of BXH-2 DNA showed that BXH-2 mice carry three endogenous MRV-related proviruses. One provirus, *Mrv5*, maps to the Y chromosome and is carried by most inbred-strain Y chromosomes that are of *M. musculus* origin. The other two BXH-2 MRV-related proviruses, *Mrv1* and *Mrv4*, are autosomal. Only one of the BXH-2 MRV-related proviruses, *Mrv1*, carries both the *env* and *pol* deletions, suggesting that the defective *Evi-2* provirus is derived from *Mrv1*. Sequence analysis of *Mrv1* is consistent with this prediction, as the sequences of *Mrv1* and the defective *Evi-2* provirus are nearly identical. The MAIDS virus must also have originated, in part, from *Mrv1*. The original source of the MAIDS virus was the Duplan-Laterjet strain of radiation leukemia virus, derived from a nonthymic lymphoma arising in an X-irradiated C57BL/6 mouse (33). C57BL/6J mice, like BXH-2 mice, transmit a single *env pol* mutant provirus, namely, *Mrv1*.

Despite the similarities we observed between MRV (*Mrv1*) and the MAIDS virus, the MAIDS virus has a number of distinguishing differences from MRV. These differences include a number of point mutations and small deletions not found in MRV. The MAIDS virus also carries unique sequences within the C-terminal end of $p15^{gag}$ and $p12^{gag}$, as well as an ecotropic LTR rather than the xenotropic LTR found in MRV. These differences most likely reflect the fact that the MAIDS virus is a recombinant virus derived from *Mrv1* and at least two other viruses. One virus appears to represent the MAIDS ecotropic virus helper, which is the probable donor of the MAIDS virus LTR. A second virus, which is carried as an endogenous virus in the mouse genome (8, 30), is thought to have donated the unique MAIDS virus *gag* sequences.

C57BL/6J mice infected with the MAIDS virus develop a syndrome that has many features in common with human AIDS, including early polyclonal proliferation of T and B cells, hypergammaglobulinemia, enhanced expression of gamma interferon, and development of B- and T-cell lymphomas (10, 12, 23, 28, 31, 49). The pathogenic determinants of the MAIDS virus map to the $p15^{gag}$ and $p12^{gag}$ regions (29, 39). MAIDS virus *gag* is expressed as a 60-kDa ($Pr60^{gag}$) polyprotein that is phosphorylated and myristylated but, in contrast to other viral *gag* polyproteins, is not processed efficiently and is membrane associated (21, 22). It has been suggested that this membrane-bound $Pr60^{gag}$ stimulates B- and T-cell proliferation by acting as a superantigen for Vb5 and Vb11 T cells (24, 27, 44). However, recent studies by Huang and Jolicoeur (22) showing that a myristylation-negative mutant of the MAIDS virus is unable to induce expansion of infected cells and is nonpathogenic suggest that MAIDS virus $Pr60^{gag}$ does not function as a superantigen. Instead, MAIDS virus $Pr60^{gag}$ may induce proliferation of infected cells by interacting with other membrane-bound effectors, which could lead to the secretion of some factor(s) detrimental to the immune system or stop the secretion of some factor(s) essential for normal functioning of the immune system.

The fact that MRV does not carry the unique $p12^{gag}$ and $p15^{gag}$ sequences found in the MAIDS virus is consistent with the hypothesis that MRV induces disease by a different mechanism, namely, insertional mutagenesis. While a number of models can be envisioned to explain the selection of somatic MRV proviruses at *Evi-2*, one model we are currently investi-

TABLE 3. *Mrv5* is carried on an *M. musculus* Y chromosome

Mrv5	Inbred strain(s)	Y chromosome origin
+	A/HeJ, AU/SsJ, BALB/cByJ, BDP/J, C3H/HeJ, C57BL/6J, C57BR/cdJ, C57L/J, C58/J, CBA/CaJ, CBA/J, CE/J, DA/HuSn, DBA/1J, DBA/2J, FS/Ei, HRS/J, I/LnJ, LP/J, NZB/B1NJ, P/J, RIIIS/J, SEA/GnJ, SEC/1ReJ	*M. musculus*
−	AKR/J, MA/MyJ, PL/J, RF/J	*M. domesticus*
−	C57BL/10J	*M. musculus*

gating assumes that this selection stems from the fact that *Evi-2* encodes a tumor suppressor gene (*Nf1*) rather than a dominantly acting oncogene. For a tumor suppressor gene to be oncogenic, both alleles must be inactivated. This is a different situation from that of a dominantly acting oncogene, in which only one allele needs to be altered for tumor formation to occur. Inactivation of both *Nf1* alleles could occur by two independent viral integrations; however, if the first integration involved a nondefective ecotropic virus, viral interference could be established, preventing a second round of viral infection and integration. Consistent with this hypothesis, we have identified a number of primary BXH-2 tumors and cell lines with integrations in both *Evi-2* alleles, and in each case, an ecotropic virus is integrated in one allele and an MRV is integrated in the second allele (7, 32). In a related model, MRV proviruses may be better able to affect normal transcription when integrated into the coding region of a tumor suppressor gene than are full-length ecotropic proviruses. If either or both of these alternative models prove correct, it may be possible to use the MRV-specific probes described here to identify other common viral integration sites that harbor tumor suppressor genes.

ACKNOWLEDGMENTS

This work was supported in part by the National Cancer Institute, DHHS, under contract NO1-CO-46000 with ABL (N.G.C. and N.A.J.) and grant CA31102 (H.G.B.). D.A.L. is a Leukemia Society of America fellow.

REFERENCES

1. **Amanuma, H., F. Laigret, M. Nishi, Y. Ikawa, and A. S. Khan.** 1988. Identification of putative endogenous proviral templates for progenitor mink cell focus-forming (MCF) MuLV-related RNAs. Virology **164:**556–561.
2. **Aziz, D. C., Z. Hanna, and P. Jolicoeur.** 1989. Severe immunodeficiency disease induced by a defective murine leukemia virus. Nature (London) **338:**505–508.
3. **Bedigian, H. G., D. A. Johnson, N. A. Jenkins, N. G. Copeland, and R. Evans.** 1984. Spontaneous and induced leukemias of myeloid origin in recombinant inbred BXH mice. J. Virol. **51:**586–594.
4. **Bedigian, H. G., L. A. Shepel, and P. C. Hoppe.** 1993. Transplacental transmission of a leukemogenic murine leukemia virus. J. Virol. **67:**6105–6109.
5. **Bedigian, H. G., B. A. Taylor, and H. Meier.** 1981. Expression of murine leukemia viruses in the highly lymphomatous BXH-2 recombinant inbred mouse strain. J. Virol. **39:**632–640.
6. **Berns, A.** 1991. Tumorigenesis in transgenic mice: identification and characterization of synergizing oncogenes. J. Cell. Biochem. **47:**130–135.
7. **Buchberg, A. M., H. G. Bedigian, N. A. Jenkins, and N. G. Copeland.** 1990. *Evi-2*, a common integration site involved in murine myeloid leukemogenesis. Mol. Cell. Biol. **10:**4658–4666.
8. **Casabianca, A., and M. Magnani.** 1994. A p12 *gag* gene homologue is present in the mouse genome. Biochem. Mol. Biol. Int. **32:**691–696.
9. **Chattopadhyay, S. K., M. R. Lander, E. Rands, and D. R. Lowy.** 1980. Structure of endogenous murine leukemia virus DNA in mouse genomes. Proc. Natl. Acad. Sci. USA **77:**5774–5778.
10. **Chattopdahyay, S. K., H. C. Morse III, M. Makino, S. K. Ruscetti, and J. W. Hartley.** 1989. Defective virus is associated with induction of murine retrovirus-induced immunodeficiency syndrome. Proc. Natl. Acad. Sci. USA **86:** 3862–3866.
11. **Chattopadhyay, S. K., D. N. Sengupta, T. N. Fredrickson, H. C. Morse III, and J. W. Hartley.** 1991. Characteristics and contributions of defective, ecotropic, and mink cell focus-inducing viruses involved in a retrovirus-induced immunodeficiency syndrome of mice. J. Virol. **65:**4232–4241.
12. **Cheung, S. C., S. K. Chattopadhyay, H. C. Morse III, and P. M. Pitha.** 1991. Expression of defective virus and cytokine genes in murine AIDS. J. Virol. **65:**823–828.

12a. **Cho, B. C.** Unpublished data.

12b. **Cho, B. C., N. A. Jenkins, and N. G. Copeland.** Unpublished data.

13. **Davisson, M.** 1986. Symbol change for *Env* and *Xp* loci. Mouse Newsl. **75:**5.
14. **Devereux, J., P. Haeberli, and O. Smithies.** 1984. A comprehensive set of sequence analysis programs for the VAX. Nucleic Acids Res. **12:**387–395.
15. **Dougherty, J. P., and H. Temin.** 1988. Determination of the rate of base-pair substitution and insertion mutations in retrovirus replication. J. Virol. **62:** 2817–2822.
16. **Frankel, W. N., J. P. Stoye, B. A. Taylor, and J. M. Coffin.** 1989. Genetic analysis of endogenous xenotropic murine leukemia viruses: association with two common mouse mutations and the viral restriction locus *Fv-1*. J. Virol. **63:**1763–1774.
17. **Frankel, W. N., J. P. Stoye, B. A. Taylor, and J. M. Coffin.** 1990. A linkage map of endogenous murine leukemia proviruses. Genetics **124:**221–236.
18. **Fredholm, M., P. F. Policastro, and M. C. Wilson.** 1991. The dispersion of defective endogenous murine retroviral elements suggests retrotransposition-mediated amplification. DNA Cell Biol. **10:**713–722.
19. **Gutmann, D. H., and F. S. Collins.** 1993. The neurofibromatosis type 1 gene and its protein product, neurofibromin. Neuron **10:**335–343.
20. **Herr, W.** 1984. Nucleotide sequence of AKV murine leukemia virus. J. Virol. **49:**471–478.
21. **Huang, M., and P. Jolicoeur.** 1990. Characterization of the *gag*/fusion encoded by the defective Duplan retrovirus inducing murine acquired immunodeficiency syndrome. J. Virol. **64:**5764–5772.
22. **Huang, M., and P. Jolicoeur.** 1994. Myristylation of $Pr60^{gag}$ of the murine AIDS-defective virus is required to induce disease and notably for the expansion of its target cells. J. Virol. **68:**5648–5655.
23. **Huang, M., C. Simard, D. G. Kay, and P. Jolicoeur.** 1991. The majority of cells infected with the defective murine AIDS virus belong to the B-cell lineage. J. Virol. **65:**6562–6571.
24. **Hügin, A. W., M. S. Vacchio, and H. C. Morse III.** 1991. A virus-encoded "superantigen" in a retrovirus-induced immunodeficiency syndrome of mice. Science **252:**424–427.
25. **Ihle, J. N., K. Morishita, T. Matsugi, and C. Bartholomew.** 1990. Insertional mutagenesis and transformation of hematopoietic stem cells. Prog. Clin. Biol. Res. **352:**329–337.
26. **Jenkins, N. A., N. G. Copeland, B. A. Taylor, H. G. Bedigian, and B. K. Lee.** 1982. Ecotropic murine leukemia virus DNA content of normal and lymphomatous tissues of BXH-2 recombinant inbred mice. J. Virol. **42:**379–388.
27. **Kanagawa, O., B. A. Nussrallah, M. E. Wiebenga, K. M. Murphy, H. C. Morse III, and F. R. Carbone.** 1992. Murine AIDS superantigen reactivity of the T cells bearing Vb5 T cell antigen receptor. J. Immunol. **149:**9–16.
28. **Klinken, S. P., T. N. Fredrickson, J. W. Hartley, R. A. Yetter, and H. C. Morse III.** 1988. Evolution of B cell lineage lymphomas in mice with a retrovirus-induced immunodeficiency syndrome, MAIDS. J. Immunol. **140:** 1123–1131.
29. **Kubo, Y., K. Kakimi, K. Higo, L. Wang, H. Kobayashi, K. Kuribayashi, T. Masuda, T. Hirama, and A. Ishimoto.** 1994. The $p15^{gag}$ and $p12^{gag}$ regions are both necessary for the pathogenicity of the murine AIDS virus. J. Virol. **68:**5532–5537.
30. **Kubo, Y., Y. Nakagawa, K. Kakimi, H. Matsui, K. Higo, L. Wang, H. Kobayashi, T. Hirama, and A. Ishimoto.** 1994. Molecular cloning and characterization of a murine AIDS virus-related endogenous transcript expressed in C57BL/6J mice. J. Gen. Virol. **75:**881–888.
31. **Kubo, Y., Y. Nakagawa, K. Kakimi, H. Matsui, M. Iwashiro, K. Kuribayashi, T. Masuda, H. Hiai, T. Hirama, S.-I. Yanagawa, and A. Ishimoto.** 1992. Presence of transplantable T-lymphoid cells in C57BL/6 mice infected with murine AIDS virus. J. Virol. **66:**5691–5695.
32. **Largaespada, D. A., J. D. Shaughnessy, Jr., N. A. Jenkins, and N. G. Copeland.** 1995. Retroviral integration at the *Evi-2* locus in BXH-2 myeloid leukemia cell lines disrupts *Nf1* expression without changes in steady-state Ras-GTP levels. J. Virol. **69:**5095–5102.
33. **Laterjet, R., and J. F. Duplan.** 1962. Experiments and discussion on leukemogenesis by cell-free extracts of radiation-induced leukemia in mice. Int. J. Radiat. Biol. Relat. Stud. Phys. Chem. Med. **5:**339–344.
34. **Manly, K. F.** 1993. A Macintosh program for storage and analysis of experimental genetic mapping data. Mamm. Genome **4:**303–313.
35. **O'Connell, P., D. Viskochil, A. M. Buchberg, J. Fountain, R. M. Cawthon, M. Culver, J. Stevens, D. C. Rich, D. H. Ledbetter, M. Wallace, J. C. Carey, N. A. Jenkins, N. G. Copeland, F. S. Collins, and R. While.** 1990. The human homologue of murine *Evi2* lies between two translocation breakpoints associated with von Recklinghausen neurofibromatosis. Genomics **7:**547–554.
36. **O'Neill, R. R., C. E. Buckler, T. S. Theodore, M. A. Martin, and R. Repaske.** 1985. Envelope and long terminal repeat sequences of a cloned infectious NZB xenotropic murine leukemia virus. J. Virol. **53:**100–106.
37. **Peters, G.** 1990. Oncogenes at viral integration sites. Cell Growth Differ. **1:**503–510.
38. **Policastro, P. F., Fredholm, M., and M. C. Wilson.** 1989. Truncated *gag* products encoded by *Gv-1*-responsive endogenous retrovirus loci. J. Virol. **63:**4136–4147.
39. **Pozsgay, J. M., M. W. Beilharz, B. D. Wines, A. D. Hess, and P. M. Pitha.** 1993. The MA (p15) and p12 regions of the *gag* gene are sufficient for the pathogenicity of the murine AIDS virus. J. Virol. **67:**5989–5999.
40. **Quint, W., W. Boelens, P. van Wezenbeek, T. Cuypers, E. R. Maandag, G. Selten, and A. Berns.** 1984. Generation of AKR mink cell focus-forming viruses: a conserved single-copy xenotrope-like provirus provides recombinant long terminal repeat sequences. J. Virol. **50:**432–438.
41. **Sambrook, J., E. F. Fritsch, and T. Maniatis.** 1989. Molecular cloning: a laboratory manual, 2nd ed. Cold Spring Harbor Laboratory Press, Cold Spring Harbor, N.Y.
42. **Sanger, F., S. Nicklen, and A. R. Coulson.** 1977. DNA sequencing with chain-terminating inhibitors. Proc. Natl. Acad. Sci. USA **74:**5463–5467.

43. **Schowalter, D. B., and S. S. Sommer.** 1989. The generation of radiolabeled DNA and RNA probes with polymerase chain reaction. Anal. Biochem. **117:**90–94.
44. **Selvey, L. A., H. C. Morse III, L. G. Granger, and R. J. Hodes.** 1993. Preferential expansion and activation of $Vb5^+$ $CD4^+$ T cells in murine acquired immunodeficiency syndrome. J. Immunol. **151:**1712–1722.
45. **Shannon, K. M., P. O'Connell, G. A. Martin, D. Paderanga, K. Olson, P. Dinndorf, and F. McCormick.** 1994. Loss of the normal *NF1* allele from the bone marrow of children with type 1 neurofibromatosis and malignant myeloid disorders. N. Engl. J. Med. **330:**597–601.
46. **Shannon, K. M., J. Watterson, P. Johnson, P. O'Connell, B. Lange, N. Shah, P. Steinherz, Y. W. Kan, and J. R. Priest.** 1992. Monosomy 7 myeloproliferative disease in children with neurofibromatosis type 1: epidemiology and molecular analysis. Blood **79:**1311–1318.
47. **Shaughnessy, J. D., F. Wiener, K. Huppi, J. F. Mushinski, and M. Potter.** 1994. A novel c-myc-activating reciprocal T(12;15) translocation juxtaposes Sa to *Pvt*-1 in a mouse plasmacytoma. Oncogene **9:**247–253.
48. **Silver, J.** 1985. Confidence limits for estimates of gene linkage based on analysis of recombinant inbred strains. J. Hered. **76:**436–440.
49. **Simard, C., M. Huang, and P. Jolicoeur.** 1994. Murine AIDS is initiated in the lymph nodes draining the site of inoculation, and the infected B cells influence T cells located at distance, in noninfected organs. J. Virol. **68:**1903–1912.
50. **Tsao, S. G. S., C. F. Brunk, and R. E. Pearlman.** 1983. Hybridization of nucleic acids directly in agarose gels. Anal. Biochem. **131:**365–372.
51. **Tucker, P. K., B. K. Lee, B. L. Lundrigan, and E. M. Eicher.** 1992. Geographic origin of the Y chromosome in "old" inbred strains of mice. Mamm. Genome **3:**254–261.
52. **van Lohuizen, M., and A. Berns.** 1990. Tumorigenesis by slow-transforming retroviruses—an update. Biochim. Biophys. Acta **1032:**213–235.
53. **Viskochil, D., A. M. Buchberg, G. Xu, R. M. Cawthon, J. Stevens, R. K. Wolff, M. Culver, J. C. Carey, N. G. Copeland, N. A. Jenkins, R. White, and P. O'Connell.** 1990. Deletions and a translocation interrupt a cloned gene at the neurofibromatosis type 1 locus. Cell **62:**187–192.